SCATTERING OF SH-WAVE BY INTERFACE CYLINDRICAL ELASTIC INCLUSION WITH DIAMETRICAL CRACKS

Jing GUO, Hui QI, Qingzhan XU

Professor, Dept. of Civil Engineering College, Harbin Engineering University, Harbin. China
Email: qihui205@sina.com, shiyong_1983@126.com

ABSTRACT :

The scattering and the dynamic stress intensity factor of SH-wave by interface cylindrical elastic inclusion with diametrical cracks are studied by the use of Green's function method. The Green's function is an essential solution of displacement field for an elastic half space with a half cylindrical inclusion impacted by out-plane harmonic line source loading at horizontal surface. The integral equations can be obtained by the use of Green's function. The dynamic stress intensity factor are given. Numerical results are illustrated and the influences of wave number, incident wave angle, geometric feature size and combination of different media parameters upon dynamic stress intensity factor are discussed.

KEYWORDS: interface cylindrical elastic inclusion with diametrical cracks, Green's function, SH-wave scattering, dynamic stress intensity factor

1. INTRODUCTION

Interface widely exists in the natural medium, engineering materials and structures, such as underground rock, various of composite materials and the structure of combinations which are bonded together. So it is inevitably that various interfaces or defects will be formed. At the same time, the defects, under the outside load, because of the impact of stress concentration, will produce a variety of crack initiation, to become complex compound defects. Therefore, the interface fracture mechanics have became hot topic in recently decades of academic research. Especially with the wider use of composite materials in recent years, these defects and cracks which are in the role of interaction of elastic waves have drawn more and more people's attention.

It has accumulated a great deal of research results to study the defects of interface. In recent years, the problems which are a series of defects of interface are discussed in detail by Diankui Liu etc., which is a new theory analysis. On the basis of this, the scattering problems of SH-waves by interface circular elastic inclusion with radial cracks are studied deeply by using the Green's function method in this paper. At the same time, the solutions of dynamic stress intensity factors at crack tip are obtained.

2. CONSTRUCTION OF GREEN'S FUNCTION

The Green's function studied is the solution of displacement field for an elastic half space with a half cylindrical inclusion impacted by out-plane harmonic line source loading at horizontal surface. The Green's function can be expressed as

when $|r_0| > R_0$,

$$G(r,r_0,\theta,\theta_0)=\begin{cases}\dfrac{i}{2\mu}H_0^{(1)}(K|r-r_0|)+\sum\limits_{m=0}^{\infty}A_m H_m^{(1)}(Kr)\cos m\theta, r>R_0\\ \sum\limits_{m=0}^{\infty}B_m J_m(K_3 r)\cos m\theta, r<R_0\end{cases} \tag{2.1}$$

when $|r_0| < R_0$,

$$G(r,r_0,\theta,\theta_0)=\begin{cases}\sum_{m=0}^{\infty}C_m H_m^{(1)}(Kr)\cos m\theta, r>R_0\\ \frac{i}{2\mu_3}H_0^{(1)}(K_3|r-r_0|)+\sum_{m=0}^{\infty}D_m J_m(K_3 r)\cos m\theta, r<R_0\end{cases} \tag{2.2}$$

where,

$$A_m=\frac{i\varepsilon_m\cos m\theta_0 H_m^{(1)}(Kr_0)\left(\mu_3K_3J_m(KR_0)J'_m(K_3R_0)-\mu KJ'_m(KR_0)J_m(K_3R_0)\right)}{2\mu\left(\mu KH'^{(1)}_m(KR_0)J_m(K_3R_0)-\mu_3K_3H_m^{(1)}(KR_0)J'_m(K_3R_0)\right)}$$

$$B_m=\frac{iK\varepsilon_m\cos m\theta_0 H_m^{(1)}(Kr_0)\left(H'^{(1)}_m(KR_0)J_m(KR_0)-H_m^{(1)}(KR_0)J'_m(KR_0)\right)}{2\left(\mu KH'^{(1)}_m(KR_0)J_m(K_3R_0)-\mu_3K_3H_m^{(1)}(KR_0)J'_m(K_3R_0)\right)}$$

$$C_m=\frac{iK_3\varepsilon_m\cos m\theta_0 J_m(K_3r_0)\left(H'^{(1)}_m(K_3R_0)J_m(K_3R_0)-H_m^{(1)}(K_3R_0)J'_m(K_3R_0)\right)}{2\left(\mu KH'^{(1)}_m(KR_0)J_m(K_3R_0)-\mu_3K_3H_m^{(1)}(KR_0)J'_m(K_3R_0)\right)}$$

$$D_m=\frac{i\varepsilon_m\cos m\theta_0 J_m(K_3r_0)\left(\mu_3K_3H'^{(1)}_m(K_3R_0)H_m^{(1)}(KR_0)-\mu KH'_m(KR_0)H_m^{(1)}(K_3R_0)\right)}{2\mu_3\left(\mu KH'^{(1)}_m(KR_0)J_m(K_3R_0)-\mu_3K_3H_m^{(1)}(KR_0)J'_m(K_3R_0)\right)}$$

in which $k=\omega/c_s$ is wave number, while ω and $c_s=\sqrt{\mu/\rho}$ are the disturbing circular frequency and the shearing velocity of the medium, ρ and μ are the mass body density and the shearing modulus of the medium, respectively.

3. SCATTERING OF SH-WAVE BY INTERFACE CYLINDRICAL ELASTIC INCLUSION WITH RADIAL CRACKS

3.1 The Model of Problem and the Boundary Conditions

As shown in figure 1, the model of interface cylindrical elastic inclusion with radial cracks is impacted by a steady incident SH-wave. The radius of cylindrical elastic inclusion is R_0, and the lengths of crack are $A1$ and $A2$ ($A1, A2 < R_0$) in left and right side of coordinate origin, respectively.

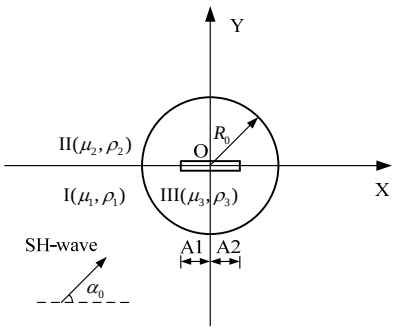

Figure 1 The mode of bi-material interface cylindrical elastic inclusion with radial cracks

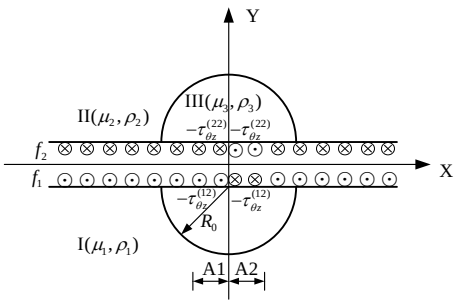

Figure 2 Forming interface cylindrical inclusion with cracks by conjunction of bi-material interface

To the problem of steady SH-wave incidence, the displacement function depends on time harmonic factor $e^{-i\omega t}$ (without considering the time harmonic factor $e^{-i\omega t}$ in the following analysis since it does not affect the outcome of the discussions). The boundary conditions of present problem should be composed of two parts, which are exterior boundary condition and interior boundary condition. To the exterior boundary condition at

far field, the *Sommerfeld* condition can be satisfied by a suitable wave function accordingly. The interior conditions should satisfy displacement continuity and stress continuity boundary conditions in interface of cylindrical elastic inclusion, and should satisfy stress freeness in two sides of crack. So the boundary conditions of the problem can be expressed as

$$\begin{cases} W^{(\mathrm{I})} = W^{(\mathrm{III})}, \tau_{rz}^{(\mathrm{I})} = \tau_{rz}^{(\mathrm{III})} \quad at \quad r = R_0, \theta \in [\pi, 2\pi) \\ 且 W^{(\mathrm{II})} = W^{(\mathrm{III})}, \tau_{rz}^{(\mathrm{II})} = \tau_{rz}^{(\mathrm{III})} \quad at \quad r = R_0, \theta \in [0, \pi) \\ \tau_{\theta z} = 0 \quad at \quad \theta = 0, \pi, r \in [0, A2] \bigcup [0, A1] \end{cases} \tag{3.1}$$

3.2 Scattering of SH-wave by Interface Cylindrical Elastic Inclusion and Radial Cracks

This paper still can be referred to the literature [7]. For the solution of bi-material interface problem, the method of "conjunction" is used to construct integral equations of SH-wave scattering. Firstly, we solve the totle displacement $W^{(1^*)}$, $W^{(2^*)}$ and the totle stress $\tau_{\theta z}^{(1^*)}, \tau_{\theta z}^{(2^*)}$ at linking section $\theta = 0, \pi$. The expressions in detials can be referred to the literature [7], in which $^* = 1, |\mathrm{r}| > R_0; ^* = 2, |\mathrm{r}| < R_0$. And θ are 0 and π, which present two integral equations, respectively.

The model of the problem is composed of two half spaces with half cylindrical inclusion, one of which is elastic half space with a half cylindrical elastic inclusion and the other is same, then we produce the modle of line-crack in length $A1 + A2$ in interface cylindrical elastic inclusion. In the program of "conjunction", the horizontal surfaces of the two half space are loaded with reverse stresses inflicted along the cracks, that is, out-of-plane harmonic line source forces $[-\tau_{\theta z}^{(22)}]$ and $[-\tau_{\theta z}^{(12)}]$, which are equal in the quantity but opposite in the direction to the stresses produced for the reason of SH-wave scattering by cylindrical elastic inclusion at the region where cracks will appear, so cracks can be made out. Then horizontal surfaces of the two half space are loaded with undetermined anti-plane forces $f_1(r_0, \theta_0)$ and $f_2(r_0, \theta_0)$ in order to satisfy displacement continuity and stress continuity conditions at linking section. So a series of *Fredholm* integral equations of first kind for determining the unknown forces can be set up through continuity conditions that are expressed in terms of the Green's function.

The stress continuity conditions at linking section can be expressed as

$$\begin{gathered} \tau_{\theta z}^{(1^*)} \cdot \cos\theta + f_1(r, \theta) = \tau_{\theta z}^{(2^*)} \cdot \cos\theta + f_2(r, \theta) \\ at \quad \theta = 0, r \geq A2; \theta = \pi, r \geq A1 \end{gathered} \tag{3.2}$$

Satisfying the displacement continuity conditions at linking section, the integral equations with undetermined anti-plane forces $f_1(r_0, \theta_0)$ can be expressed as

$$\begin{aligned} &\int_{A1}^{\infty} f_1(r_0, \pi)\left[G_1(r, \theta, r_0, \pi) + G_2(r, \theta, r_0, \pi)\right] dr_0 \\ &+ \int_{A2}^{\infty} f_1(r_0, 0)\left[G_1(r, \theta, r_0, 0) + G_2(r, \theta, r_0, 0)\right] dr_0 \\ &= W^{(2^*)}(r, \theta) - W^{(1^*)}(r, \theta) \\ &+ \int_{A_1}^{\infty} [\tau_{\theta z}^{(1^*)} - \tau_{\theta z}^{(2^*)}]_{\theta=\pi} G_2(r, \theta, r_0, \pi) dr_0 - \int_{A_2}^{\infty} [\tau_{\theta z}^{(1^*)} - \tau_{\theta z}^{(2^*)}]_{\theta=0} G_2(r, \theta, r_0, 0) dr_0 \\ &- \int_0^{A_1} \left[\tau_{\theta z}^{(12)}(r_0, \pi) G_1(r, \theta, r_0, \pi) + \tau_{\theta z}^{(22)}(r_0, \pi) G_2(r, \theta, r_0, \pi)\right] dr_0 \\ &+ \int_0^{A_2} \left[\tau_{\theta z}^{(12)}(r_0, 0) G_1(r, \theta, r_0, 0) + \tau_{\theta z}^{(22)}(r_0, 0) G_2(r, \theta, r_0, 0)\right] dr_0 \end{aligned} \tag{3.3}$$

in which, θ are 0 and π, which present two integral equations, respectively. G_1 and G_2 are Green functions in media I and II, respectively.

4. DYNAMIC STRESS INTENSITY FACTORS AT CRACK TIP

Dynamic stress intensity factors at crack tip K_{III} can be expressed as

$$K_{\mathrm{III}} = \lim_{r \to A} f_1(r,\theta) \cdot \sqrt{2\pi(r-A)} \tag{4.1}$$

in which, A=A1 or A2.
In the calculation, we usually determine a non-dimensional dynamic stress intensity factor as k_3.

$$k_3 = \left| \frac{K_{\mathrm{III}}}{\tau_0 Q} \right| \tag{4.2}$$

It is the ratio which is dynamic stress intensity factor K_{III} and the corresponding static stress intensity factor $K_{\mathrm{III}}^{(s)} = \tau_0 Q$. In which, Q is a characteristic parameters with the square root of the length dimension.

In this paper, we get $Q = \sqrt{\pi A^{'} / 2}$, in which, $A^{'} = A1 + A2$ which is the length of the line-crack. τ_0 is the stress which is the largest amplitude in the direction along the direction α_0 of the incident of SH-wave, that is

$$\tau_0 = \left| \tau_{rz}^{(i)} \right| = \mu_1 K_1 W_0 \tag{4.3}$$

5. CALCULATING EXAMPLES AND DISCUSSIONS

In this paper, we analyse the influences of wave number, incident wave angle, geometric feature size and combination of different media parameters upon solutions of dynamic stress intensity factors. Where, $\mu_1^* = \mu_2 / \mu_1$, $\mu_2^* = \mu_3 / \mu_1$, $K_1^* = K_2 / K_1$, $K_2^* = K_3 / K_1$.

(1) Figure 3 and figure 4 give the results of the line-crack in length 2A of symmetry y-axis in the cylindrical elastic inclusion with radial cracks when $K_1^* = 1$, $\mu_1^* = 1$, $K_2^* = 1$, $\mu_2^* = 1$. J.F. Loeber and G.C. Sih have given the answers in use of transform integral equations for the dual approach. It can be seen from figure 3 that the changes of DSIF with wave numbers $K_1 A$ while the SH-waves are vertical incidence. In the figure, when $K_1 A = 0.95$, DSIF appears the biggest value, about 1.275. It can be seen from figure 4 that the changes of DSIF with different incident wave angles while the SH-waves incident with different angles. When SH-waves are horizontal incidence, we can obtain the value of DSIF directly which is zero from the integral equations. Hongwei Liu also obtains the results of degradation of this paper in use of Green's function in research at the cracks originating at a circular hole edge. The data in this paper is consistent with Hongwei Liu's.

(2) Figure 5 gives the results of the dynamic stress intensity factor under the different incident angle α_0 and K_2^* when, $K_1^* = 1, \mu_1^* = 1, K_1 R_0 = 0.1, \mu_2^* = 1.0, A / R_0 = 0.5$ .This example is the case of low frequency incidence. It can be seen from figure 5 that the low frequency incidence exists Low-frequency resonance phenomenon. Dynamic stress intensity factor will increase sharply to great value at some K_2^*. In addition, the peaks of dynamic stress intensity factor also reduce gradually with the decrease of the incident angle α_0. When SH-waves are horizontal incidence, its peak becomes to zero. However, it does not exist phenomenon of "resonance" when it incidents in high-frequency. So we should avoid the phenomenon of "low-frequency resonance" arose.

(3) Figure 6 gives the changes of DSIF with K_2^* at different lengths of the crack, when $K_1^* = 1$, $\mu_1^* = 1$, $K_1 R_0 = 1.0$, $\mu_2^* = 1.0$ and the SH-waves are vertical incidence. The graph shows that there are still many peaks, but they are much smaller than the peaks of low-frequency resonance. However, its peaks will decrease with the increase of A / R_0.

(4) Figure 7 gives the changes of DSIF with $K_1 R_0$ at different μ_2^*, when $K_1^* = 2$, $K_2^* = 2$, $\mu_1^* = 2$,

$A/R_0=0.5$ and the SH-waves are vertical incidence. It can be seen that the changes of volatility of DSIF in the interface cylindrical elastic inclusion with radial cracks. At the same time, it is obvious in volatility. The peaks of its DSIF also increase gradually.

(5) Figure 8 gives the changes of DSIF in different K_1^* with K_2^*, when $K_1R_0=0.1$, $\mu_1^*=2$, $\mu_2^*=2$, $A/R_0=0.5$ and the SH-waves are vertical incidence. It also can be seen that the phenomenon of the low-frequency resonance in interface inclusion. Dynamic stress intensity factor will increase sharply to great value at some K_2^*, then it will be decrease sharply in inverse proportion to the magnitude of resonance.

(6) Figure 9 gives the changes of DSIF in different μ_1^* with K_2^*, when $K_1R_0=1.0$, $K_1^*=2$, $\mu_2^*=2$, $A/R_0=0.5$ and the SH-wave are vertical incidence. Figure 10 gives the changes of DSIF in different K_1^* with K_2^*, when $K_1R_0=1.0$, $\mu_1^*=2$, $\mu_2^*=2$, $A/R_0=0.5$ and the SH-wave are vertical incidence. The graphs show that there are still many peaks and they are obvious in volatility, but it is much smaller than the peaks of low-frequency resonance. Figure 9 shows that, with the increase of μ_1^*, the value of the largest of its peaks are lower than before. At the same time, figure 10 shows that the peaks of DSIF also reduce gradually with the increase of K_1^*.

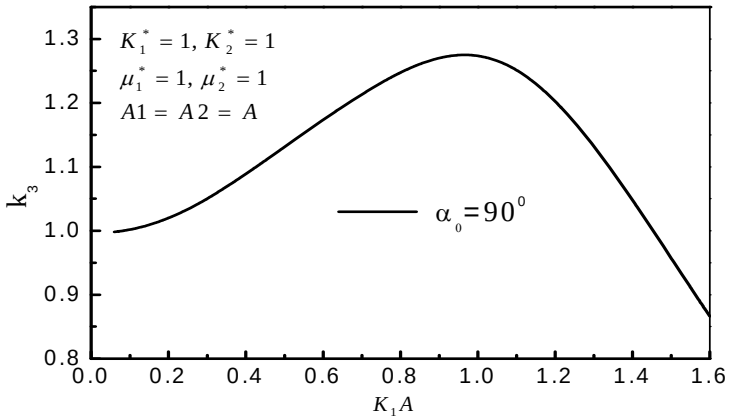

Figure 3 Variation of DSIF in homogenous medium with line crack impacted by SH-wave vertically

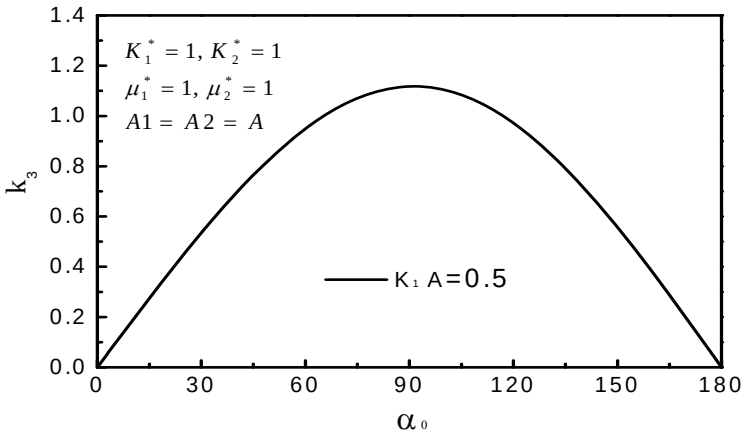

Figure 4 Variation of DSIF in homogenous medium with line crack vs. incident angle of SH-wave

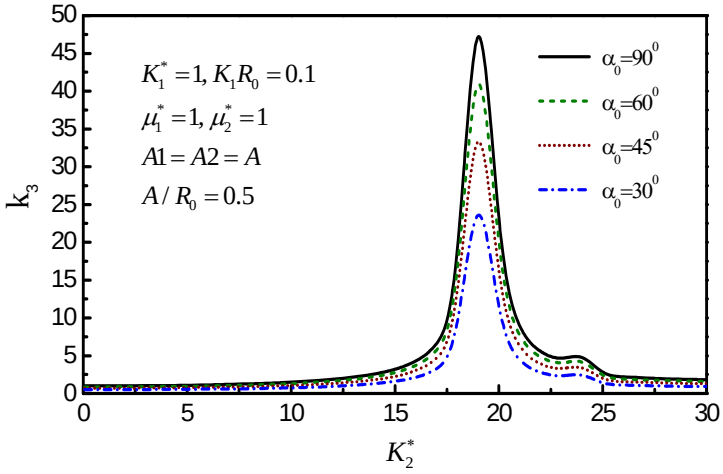

Figure 5 Variation of DSIF vs. K^* for varied α_0 and lower wave number

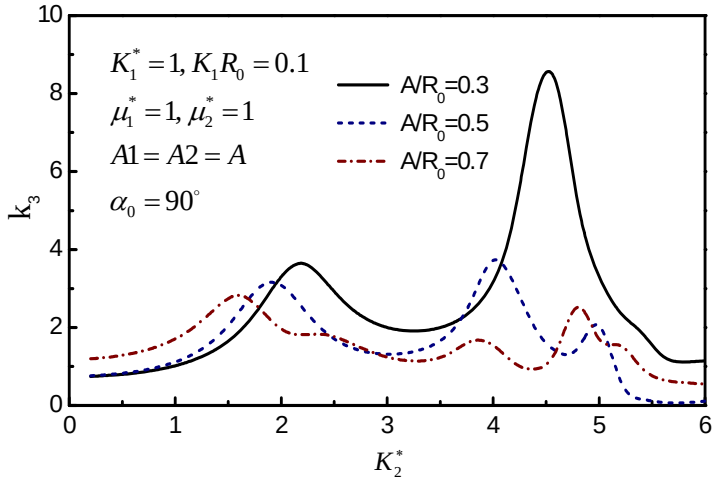

Figure 6 Variation of DSIF vs. K^* for varied A/R_0 and vertical SH-wave

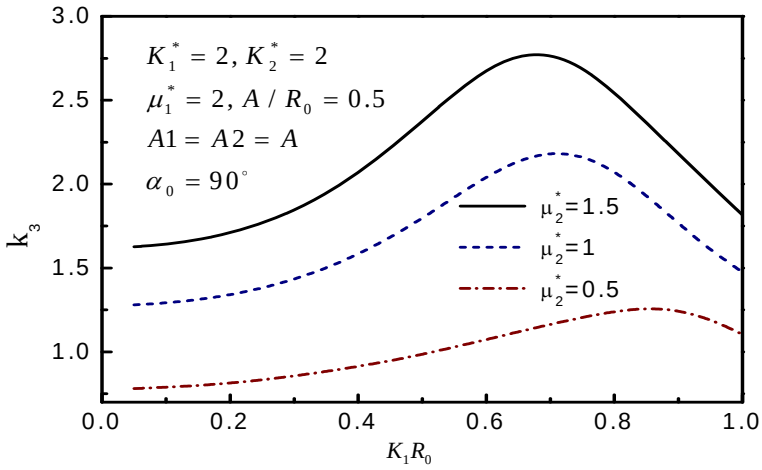

Figure 7 Variation of DSIF vs. K_1R_0 for varied μ_2^*, $\alpha_0=90^0$

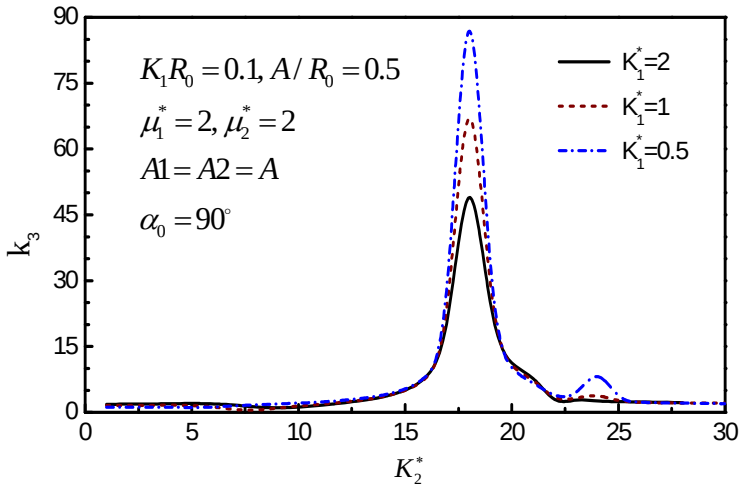

Figure 8 Variation of DSIF vs. K_2^* for varied K_1^*, $K_1R_0=0.1$

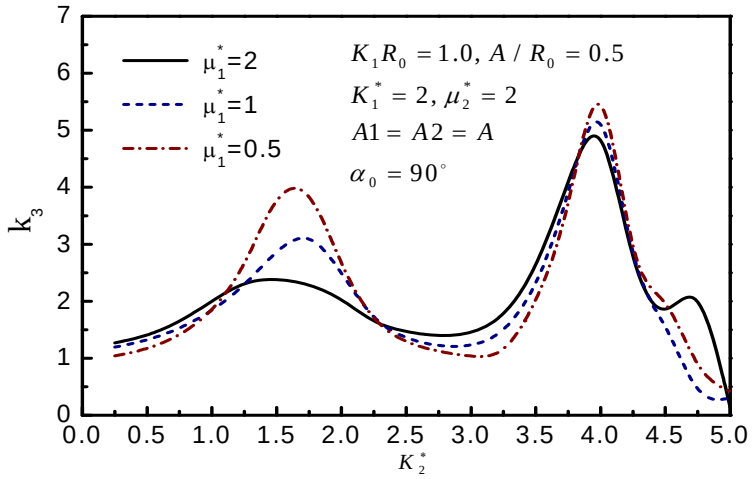

Figure 9 Variation of DSIF vs. K_2^* for varied μ_1^*, $K_1R_0=1.0$

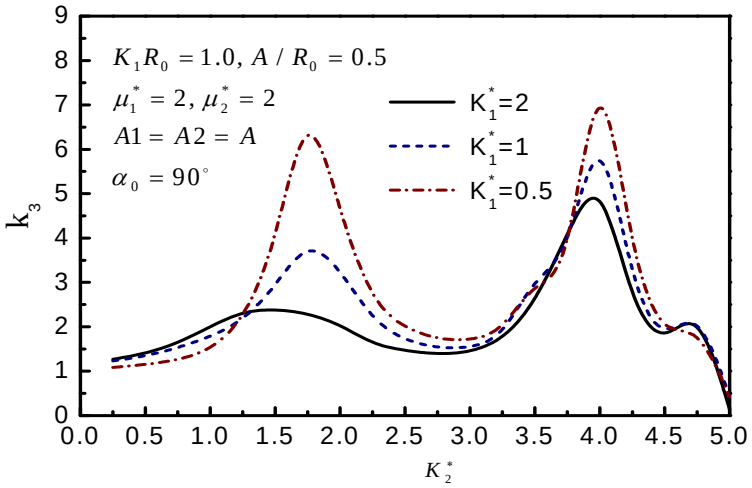

Figure 10 Variation of DSIF vs. K_2^* for varied K_1^*, $K_1R_0=1.0$

6. CONCLUSIONS

Through research, we can obtain the conclusion as follows:

(1) The changes of dynamic stress intensity factor not only have relation with the non-dimensional wave numbers, the incident angles α_0 and various of combinations of the materials, but also have relation with the ratios of feature size A/R_0 in Scattering of SH-wave by interface cylindrical elastic inclusion with diametrical cracks.

(2) Whether cylindrical elastic inclusion with diametrical cracks in uniformly medium or interface cylindrical elastic inclusion with diametrical cracks, dynamic stress intensity factors at crack tip are very strong by the influence of the non-dimensional incident wave numbers and they occur the phenomenon of the low-frequency resonance. Therefore, we should prevent the occurrence of low-frequency resonance.

REFERENCES

Pao Y.H. (1983). Elastic Waves in Solids. *ASME Journal of Applied Mechanics* **50:4,** 1152-1164

Duo Wang, Xingrui Ma, Diankui Liu. (1995). The latest Progress of the Elastic dynamics. Beijing, Publishing house of Science (in Chinese)

Diankui Liu and Hongwei Liu. The scattering of SH-wave and the dynamic stress concentration of interface near the circular hole. *Acta Mechanica Sinica* **30:5,** 597-604 (in Chinese).

Diankui Liu and Hongwei Liu. (1999). Scattering of SH-wave by cracks originating at a circular hole edge and dynamic. *Acta Mechanica Sinica* **31:3,** 292-299 (in Chinese).

Shouxia Shi and Diankui Liu. (2001). Scattering and dynamic stress concentration of SH-wave and multiple holes of interface. *Acta Mechanica Sinica*, **33:1,** 60-70 (in Chinese).

Shouxia Shi, Qingshan Yang, Diankui Liu, Hui Qi. (2000). Scattering and dynamic stress concentration of SH-wave by cylindrical inclusion and cracks. *Journal of composite materials* **17:3,** 109-112 (in Chinese).

Diankui Liu and Jiayong Tian. (1999). Scattering and dynamic stress concentration of SH-wave by interface cylindrical inclusion. *The explosion and the impact*. **19:2,** 115-123 (in Chinese).

Zhang Heng. (1992). The Solution of the stress intensity factor in fracture mechanics. *Publishing house of defense industry* (in Chinese).

J.F. Loeber and G.C. Sih. (1968). Diffraction of anti-plane shear waves by a finite crack. *Journal of the Acoustical Society of America* **44:1,** 90-98